Investigation of the *Methanosarcina thermophila* Acetate Kinase Mechanism by Fluorescence Quenching†

Andrea Gorrell‡ and James G. Ferry*

Department of Biochemistry and Molecular Biology, Pennsylvania State University, University Park, Pennsylvania 16802

Received June 30, 2007; Revised Manuscript Received October 5, 2007

ABSTRACT: Acetate kinase, a member of the acetate and sugar kinase/Hsc 70/actin (ASKHA) structural superfamily, catalyzes the reversible transfer of the γ-phosphoryl group from ATP to acetate, yielding ADP and acetyl phosphate. A catalytic mechanism for the enzyme from *Methanosarcina thermophila* has been proposed on the basis of the crystal structure and kinetic analyses of amino acid replacement variants. The $Gln^{43}Trp$ variant was generated to further investigate the catalytic mechanism via changes in fluorescence. The dissociation constants for ADP·Mg^{2+} and ATP·Mg^{2+} ligands were determined for the $Gln^{43}Trp$ variant and double variants generated by replacing Arg^{241} and Arg^{91} with Ala and Lys. The dissociation constants and kinetic analyses indicated roles for the arginines in transition state stabilization for catalysis but not in nucleotide binding. The results also provide the first experimental evidence for domain motion and evidence that catalysis does not occur as two independent active sites of the homodimer but the active site activities are coordinated in a half-the-sites manner.

Acetate kinase (EC 2.7.2.1) is a homodimer which catalyzes the reversible magnesium-dependent transfer of the γ-phosphoryl group from ATP to acetate, yielding ADP and acetyl phosphate ($CH_3COO^- + ATP \leftrightarrow CH_3CO_2PO_3^{2-} + ADP$). The enzyme is widely distributed among fermentative prokaryotes in the bacteria domain where it functions together with phosphotransacetylase ($CH_3CO_2PO_3^{2-} + HS\text{-}CoA \leftrightarrow CH_3COSCoA + HPO_4^{2-}$) to convert acetyl-CoA to acetate and synthesize ATP. These enzymes also function to activate acetate to acetyl-CoA in the first step of the pathway for conversion of the methyl group to methane by *Methanosarcina* species from the Archaea domain (*1*).

Though acetate kinase was one of the earliest phosphoryl transfer enzymes to be identified (*2*) and investigated, a debate persisted in the literature until recently about whether the catalytic mechanism is a triple displacement of the phosphate involving two covalent enzyme intermediates (*3*) or a direct in-line phosphoryl transfer (*4, 5*). Support for the direct in-line mechanism accrues from studies with the acetate kinase from *Methanosarcina thermophila* (*6*−*12*). The enzyme cocrystallized with ADP, Al^{3+}, F^-, and acetate shows an ADP−AlF_3−acetate linear array in the active site cleft wherein the AlF_3 is proposed to mimic the *m*-phosphate transition state (*11*). Kinetic analyses of Arg^{241} and Arg^{91} replacement variants indicate these active site residues are essential for catalysis and important for binding acetate (*11*). In a direct in-line phosphoryl transfer, the hypothesized transition state is a trigonal bipyramidal structure of the γ-phosphoryl group, with the axial positions occupied by β-phosphoryl and acetyl oxygens. The guanidino groups of Arg^{241} and Arg^{91} are proposed to stabilize this structure by interacting with oxygen atoms of the γ-phosphoryl and carboxyl groups of acetate (*11*). The guanidino group of Arg^{241} is adjacent to AlF_3, consistent with the proposed role. However, the guanidino group of Arg^{91} is displaced 7 Å from AlF_3, casting doubt on the proposed role, although the structure may not accurately represent the position of Arg^{91} during catalysis (*11*).

On the basis of structural similarities of the *M. thermophila* enzyme, acetate kinase was identified as a member of the acetate and sugar kinase/Hsc70/actin (ASKHA)[1] structural superfamily (*12*). Each monomer of the homodimeric acetate kinase is characterized by a duplicated central β-sheet surrounded by α-helices ($\beta\beta\beta\alpha\beta\alpha\beta\alpha$ core) and consisting of two domains (Figure 1). The sugar kinase and actin family members are all known to undergo a catalytically essential domain closure upon ligand binding (*13*−*18*). Although there is no experimental evidence to support domain closure during catalysis of acetate kinase from *M. thermophila*, domain closure has been suggested to participate in stabilization of the transition state based upon the architecture of the crystal structure (*12*).

The *M. thermophila* acetate kinase has no tryptophan residues which has precluded intrinsic fluorescence measurements as an approach to investigating the catalytic mechanism. Here we report K_d values for ADP·Mg and ATP·Mg ligands for the *M. thermophila* acetate kinase enabled by fluorescence quenching of the $Gln^{43}Trp$ variant. Double variants, with either Arg^{241} or Arg^{91} replaced in the $Gln^{43}Trp$ variant, had K_d values consistent with previously proposed

† This work was supported by National Institutes of Health Grant GM44661 to J.G.F.

* To whom correspondence should be addressed: Department of Biochemistry and Molecular Biology, Pennsylvania State University, University Park, PA 16082. Telephone: (814) 863-5721. Fax: (814) 863-6217. E-mail: jgf3@psu.edu.

‡ Current address: Chemistry Program, University of Northern British Columbia, Prince George, BC V2M 4Z9, Canada.

[1] Abbreviations: ASKHA, acetate and sugar kinase/Hsc70/actin; AK, acetate kinase; AcP, acetyl phosphate; Ac, acetate.

10.1021/bi701292a CCC: $37.00
Published on Web 11/14/2007

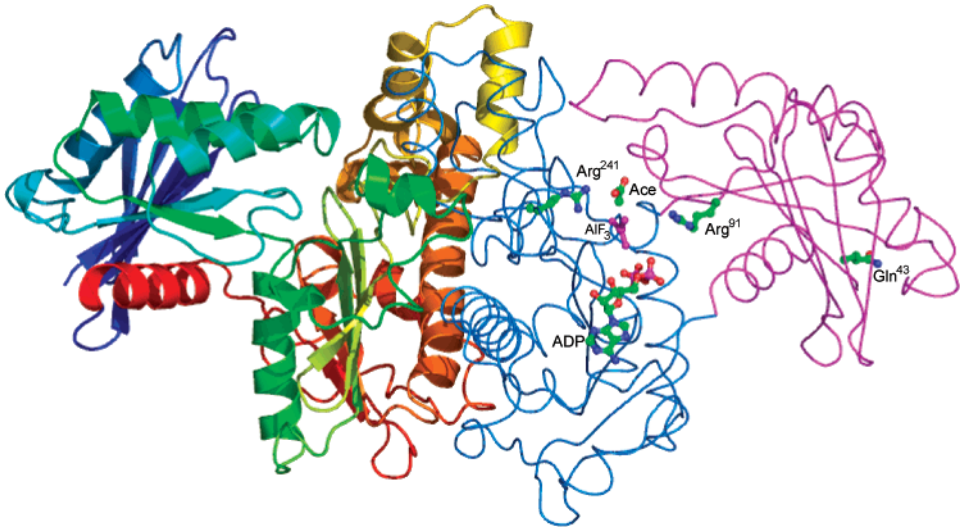

FIGURE 1: Structure of the *M. thermophila* acetate kinase [1TUY (*11*)]. The dimer is shown with monomer A (ribbon representation) in rainbow hue from the blue N-terminus to the red C-terminus. Monomer B (wire representation) with domain I (residues 1−148 and 383−398) colored marine and domain II (residues 149−382) colored magenta. Shown in ball-and-stick representation in monomer B are the active site Arg^{91} and Arg^{241} residues in CPK colors, and transition state analogue components ADP, AlF_3, and acetate in CPK colors except Al (orange) and F (cyan). Residue Gln^{43} is shown in ball-and-stick colored CPK in domain I of monomer B.

roles for these arginines in catalysis and substrate binding. The Gln^{43}Trp variant has also provided evidence for domain motion with implications for the catalytic mechanism. The results indicate that catalysis does not occur as two independent active sites but that the active site activities are coordinated in a half-the-sites manner.

MATERIALS AND METHODS

Materials. Chemicals were purchased from Sigma Chemical, VWR Scientific Products, or Fisher Scientific. Oligonucleotides for DNA sequencing and site-directed mutagenesis were purchased from Integrated DNA Technologies (Coralville, IA). ATP and ADP solutions were adjusted to pH 7.0 with sodium hydroxide and concentrations determined utilizing the extinction coefficient ($\epsilon_{259} = 15.4 \times 10^3$ M^{-1} cm^{-1}). All ATP and ADP solutions were equimolar with magnesium chloride. Acetate (Ac) stock solutions were adjusted to pH 7.0 with sodium hydroxide. Acetyl phosphate (AcP) solutions were made fresh daily, and concentrations were verified via a kinetic assay (*19*) from the maximal change in absorbance.

Site-Directed Mutagenesis. Mutagenesis was performed by the oligonucleotide-directed in vitro mutagenesis method (*20*) using the QuikChange mutagenesis kit (Stratagene). The plasmid pET-AK, a derivative of pET-15b with the *M. thermophila ack* gene from pML703 (*21*) in the multicloning site (*7*), was the target for mutagenesis. Mutations were verified by dye termination cycle sequencing using an ABI PRISM 377 DNA sequencer (Applied Biosystems) at the Nucleic Acid Facility at Pennsylvania State University.

Heterologous Production and Purification of Acetate Kinases. The wild-type and variant acetate kinases were overproduced in *Escherichia coli* BL21(DE3) [F^- *dcm ompT hsdS* ($r_B^-m_B^-$) *gal* λ(DE3)] and purified as described previously (*21*). All variants were further purified via gel filtration in a 100 mL Sephadex G-200 column (1.6 cm diameter) at a flow rate of 1.0 mL/min. Protein purity was examined by SDS−polyacrylamide gel electrophoresis (*22*), and protein concentrations were determined by the Bradford method (*23*) using Bio-Rad dye reagent with bovine serum albumin as the standard.

Kinetic Parameters of Wild-Type and Variant Acetate Kinases. Kinetic parameters for wild-type and variant acetate kinases were determined as previously described with assays performed utilizing the coupled assay systems for both the ADP/AcP-synthesizing (*11*) and ATP/Ac-synthesizing (*19*, *24*) reaction directions holding the concentration of the nonvariable substrate at 10 times its K_m. Data were fit using nonlinear regression analysis (Kaleidagraph, Synergy Software), with the exception of the Arg^{91}Ala/Gln^{43}Trp variant. Due to the inability to saturate substrate at 5 M acetate for the Arg^{91}Ala/Gln^{43}Trp variant, when $K_m^{ATP\cdot Mg}$ was determined data were fit using Lineweaver−Burk regression anaysis, holding acetate at 2 M.

Steady-State Fluorescence Measurements. The intrinsic fluorescence of wild-type and variant acetate kinases was determined using a Hitachi F-200 fluorometer and 1 cm path length cuvettes, with 0.07−1 μM enzyme, 50 mM Tris, 130 mM NaCl, and 10 mM $MgCl_2$, in a total volume of 2 mL. Initial scans of the wild-type and tryptophan variants were taken at a constant 20 °C using a circulating water bath, with 2 nm steps for both excitation and emission wavelengths with each data point an average of 10 measurements. Fluorescence was measured in arbitrary intensity units.

Equilibrium Binding Studies. The equilibrium dissociation constants (K_d) of the Gln^{43}Trp and Gln^{43}Trp double variants were determined by measuring the observed decrease in fluorescence intensity upon addition of the ligand. Ligands utilized were ATP·Mg and ADP·Mg. Buffer conditions were as described in the preceding section for steady-state fluorescence measurements, where excitation and emission wavelengths were 295 and 340 nm, respectively. Each enzyme was held at the same concentration used for the kinetic assay (see above) and was titrated with each nucleotide ligand, measuring the fluorescence intensities after an incubation time of 10 min. The time was chosen as equilibrium where no further change in fluorescence was observed. ATP·Mg hydrolysis by acetate kinase over the time

Table 1: Kinetic Parameters of Wild-Type and Variant Acetate Kinases Assayed in the Direction of ADP and Acetyl Phosphate Synthesis

enzyme	k_{cat} (s^{-1})	$K_m^{ATP\cdot Mg}$ (μM)	K_m^{Ac} (mM)
wild-type[a]	913 ± 52	80 ± 9	2.7 ± 0.3
$Gln^{43}Trp$	699 ± 24	53 ± 3	12.4 ± 0.3
$Arg^{91}Ala$[a]	0.11 ± 0.004	16 ± 0.6	250 ± 38
$Arg^{91}Ala/Gln^{43}Trp$	2.07[b]	539 ± 32[c]	12000[b]
$Arg^{91}Lys$[a]	3.7 ± 0.18	76 ± 3	70 ± 3
$Arg^{91}Lys/Gln^{43}Trp$	11.8 ± 0.53	234 ± 21	48 ± 5
$Arg^{241}Ala$[a]	0.68 ± 0.1	297 ± 27	710 ± 130
$Arg^{241}Ala/Gln^{43}Trp$	1.83 ± 0.3	80.5 ± 14	5.8 ± 0.95
$Arg^{241}Lys$[a]	1.3 ± 0.06	11400 ± 1900	77 ± 7
$Arg^{241}Lys/Gln^{43}Trp$	0.40 ± 0.05	1300 ± 130	179 ± 46

[a] Previously published (*11*). [b] From Lineweaver−Burk plots with 10 mM ATP·$MgCl_2$ as enzyme could not be saturated up to 5 M acetate. [c] From Michaelis−Menten plots with 2 M acetate.

frame of the binding studies was insignificant (data not shown). All fluorescence intensities were corrected for protein dilution.

RESULTS

Generation of the Fluorescent Variant. As the *M. thermophila* acetate kinase has no tryptophan, several residues (Tyr^{15}, Gln^{43}, Phe^{151}, and Phe^{252}) were individually replaced with tryptophan to generate variants to investigate the catalytic mechanism via fluorescence quenching. Selection of residues for replacement was based on three criteria: (i) location near the substrate binding site, (ii) space for a tryptophan residue, and (iii) probability of environmental change. Further, the *E. coli* K12 acetate kinase contains a single tryptophan residue (Trp^{46}) in the position equivalent to Gln^{43} in the *M. thermophlia* enzyme.

Wild-type and all variant enzymes were overexpressed in *E. coli* BL21(DE3) and purified to apparent homogeneity as judged by SDS−PAGE (data not shown). The yields of the purified variants were similar to that of the wild-type enzyme, and native gel filtration chromatography indicated that all variants were dimeric in accordance with the wild type (data not shown). These results indicate that the variants were not compromised by major structural changes.

The $K_m^{ATP\cdot Mg}$ and K_m^{Ac} values for the variants were compared to the wild-type values to determine the effect of the replacements on the kinetic parameters. The parameters of the $Tyr^{15}Trp$, $Phe^{151}Trp$, and $Phe^{252}Trp$ variants deviated too far from those of the wild type to be valid experimental tools (data not shown). However, the differences in kinetic parameters of the $Gln^{43}Trp$ variant versus the wild-type enzyme (Tables 1 and 2) were not large enough to preclude the use of this variant in investigating the catalytic mechanism via fluorescence quenching.

A λ_{max} for excitation of 295 nm and a λ_{max} for emission of 340 nm were determined for both the $Gln^{43}Trp$ variant and wild-type acetate kinase (Figure 2). However, the intensity of the variant was increased several-fold over that of the wild type.

Kinetic Analysis of Double-Variant Acetate Kinases. The fluorescent $Gln^{43}Trp$ variant was used to generate double variants by replacement of Arg^{91} or Arg^{241} with Ala and Lys to probe the roles of these residues. Each variant was purified to apparent homogeneity as judged by SDS−PAGE. The yields and properties of the variants were similar to those of the wild type (data not shown), indicating that the variants were not compromised by major structural changes.

Table 2: Kinetic Parameters of Wild-type and Variant Acetate Kinases Assayed in the Direction of ATP and Acetate Synthesis

enzyme	k_{cat} (s^{-1})	$K_m^{ADP\cdot Mg}$ (μM)	K_m^{AcP} (mM)
wild-type[a]	1255 ± 60	98 ± 7	0.47 ± 0.05
$Gln^{43}Trp$	2650 ± 370	173 ± 12	0.26 ± 0.06
$Arg^{91}Ala$[a]	3.5 ± 0.8	63 ± 6	1.36 ± 0.2
$Arg^{91}Ala/Gln^{43}Trp$	2.63 ± 0.3	147 ± 26	2.58 ± 0.2
$Arg^{91}Lys$[a]	23 ± 0.2	168 ± 6	0.61 ± 0.06
$Arg^{91}Lys/Gln^{43}Trp$	25.7 ± 1.7	164 ± 23	1.08 ± 0.08
$Arg^{241}Ala$[a]	4.5 ± 0.4	210 ± 28	0.84 ± 0.02
$Arg^{241}Ala/Gln^{43}Trp$	14.6 ± 1.6	239 ± 38	0.33 ± 0.03
$Arg^{241}Lys$[a]	4.5 ± 0.4	578 ± 21	0.92 ± 0.03
$Arg^{241}Lys/Gln^{43}Trp$	10.5 ± 1.3	692 ± 86	1.02 ± 0.11

[a] Previously published (*11*).

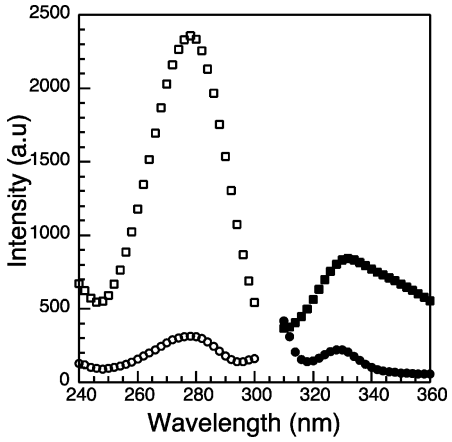

FIGURE 2: Excitation and emission spectra of acetate kinases: wild type [excitation (○) and emission (■)] and $Gln^{43}Trp$ variant [excitation (□) and emission (●)]. Scans were performed with 6.5 μg/mL protein, 50 mM Tris (pH 7.4), and 40 mM NaCl in a 1 cm path length cuvette. Excitation was monitored at 340 nm and emission at 295 nm. a.u. represents arbitrary units.

For the ADP/acetylphosphate-producing direction (Table 1), all the double variants showed a substantial decrease in k_{cat} versus the $Gln^{43}Trp$ variant commensurate with previously published values for the single Arg^{91} and Arg^{241} variants versus the wild type that further support the previously proposed role for these arginines interacting with the *m*-phosphate and stabilizing the transition state (*11*). In most cases, the trends in differences for K_m values between the double variants and the $Gln^{43}Trp$ variant were consistent with trends between the single variants and the wild type which led to the previous proposal that neither arginine binds ATP (*11*). However, exceptions were observed for the $K_m^{ATP\cdot Mg}$ of the $Arg^{91}Ala/Gln^{43}Trp$ variant and the K_m^{Ac} of the $Arg^{241}Ala/Gln^{43}Trp$ variant versus the $Gln^{43}Trp$ variant. The most straightforward explanation is that the $Gln^{43}Trp$ substitution, together with the additional space created by substituting alanine, rearranged residues affecting the binding of ATP and acetate. The $Arg^{241}Lys/Gln^{43}Trp$ variant also had a very high $K_m^{ATP\cdot Mg}$ versus the $Gln^{43}Trp$ variant, a trend consistent with the $Arg^{241}Lys$ versus wild type that was previously attributed to the larger lysine side chain sterically hindering ATP binding (*11*). Thus, the overall differences in $K_m^{ATP\cdot Mg}$ values for the double variants versus the $Gln^{43}Trp$ variant do not contradict the previous proposal that neither arginine is important for binding ATP. Finally, with the exception of the $Arg^{241}Ala/Gln^{43}Trp$ variant, the differ-

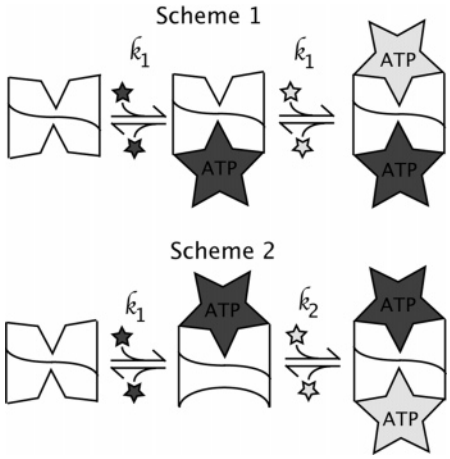

FIGURE 3: Schemes for binding of nucleotide to acetate kinase. Scheme 1 is equivalent binding to either monomer, or independent active sites. Scheme 2 is nonequivalent ligand binding where binding to one monomer affects binding to a second monomer, or coordinated active sites.

ences in K_m^{Ac} values for the double variants versus the Gln[43]-Trp variant are consistent with the previously proposed role for both arginines in binding acetate based on previously published K_m^{Ac} values for the single variants versus the wild type (*11*).

In the direction of ATP/acetate synthesis (Table 2), all the double variants exhibited large decreases in k_{cat} versus the Gln[43]Trp variant that were similar in magnitude to published values for the single variants versus the wild type that support the previously proposed roles for these arginines in catalysis (*11*). The differences in K_m values for all the double variants versus the Gln[43]Trp variant were in accord with published differences between the cognate single variants and the wild type, which led to the previous conclusion that Arg[91] and Arg[241] have no influence on binding of ADP or acetyl phosphate (*11*).

Determination of Nucleotide Binding Constants. The utility of the fluorescent Gln[43]Trp variant in probing the catalytic mechanism was assessed by determining the ability of ATP·Mg, ADP·Mg, and acetate to induce fluorescence quenching of the variant. The nucleotides alone caused quenching (data not shown), while acetate and acetyl phosphate were unable to cause quenching (data not shown).

Two possible schemes for binding of the nucleotides to the dimeric enzyme are shown in Figure 3. Scheme 1 indicates two equal independent binding sites per dimer each with the same affinity for the ligand, a version of the Stern−Volmer equation (eq 1) (*25*)

$$\frac{\Delta F}{F_o} = \frac{(\Delta F_{max}/F_o)L^n}{K_d + L^n} \quad (1)$$

where F_o is the intrinsic fluorescence, ΔF is the change in fluorescence in the presence of ligand, K_d is the dissociation constant, and L is the concentration of ligand, or quencher. The initial fit of fluorescence data to the equation of two independent sites (eq 1) showed that Scheme 1 did not fit the experimental data (data not shown). Scheme 2 indicates that binding to one site on the dimer influences binding of ligand to the second site on the dimer, an expression analogous to the Hill equation (*25*). Note that Schemes 1 and 2 (Figure 3) are for ligand binding, without enzymatic catalysis occurring. Thus, two binding sites with dissimilar equilibrium binding constants (K_{d1} and K_{d2}; Figure 3, Scheme 2) were considered for the dimeric enzyme. Consequently, the equation to fit the fluorescence data was modified to incorporate the dissimilar binding constants. In the equations that follow, F_o is the total intrinsic fluorescence, $F_{o(1)}$ and $F_{o(2)}$ are the total intrinsic fluorescence intensities attributable to each site, F is the resultant fluorescence for the whole protein, $F_{(1)}$ and $F_{(2)}$ are the resultant fluorescence for sites 1 and 2, respectively, and L is the concentration of free ligand, or quencher (*25*). The expression for dissociation of ligand at binding site 1 is given in eq i, with the expressions for total observed fluorescence (eq ii), total intrinsic fluorescence (eq iii), and observed fluorescence from each site (eq iv and eq v). Rearrangement of eq ii and substitution into eq i result in the expression for fluorescence from site 1 represented by eq vi

$$K_{d1} = \frac{F_{(1)}L}{FL} \quad (i)$$

$$F_o = F_{o(1)} + F_{o(2)} \quad (ii)$$

$$F = F_{(1)} + F_{(2)} \quad (iii)$$

$$F_{o(1)} = F_{(1)} + F_{(1)}L \quad (iv)$$

$$F_{o(2)} = F_{(2)} + F_{(2)}L_2 \quad (v)$$

$$F_{(1)} = \frac{F_{o(1)}}{1 + K_{d1}L} \quad (vi)$$

Binding to the opposite monomer is represented by expression vii

$$K_{d2} = \frac{F_{(2)}L_2}{[F_{(1)}L]L} \quad (vii)$$

and substitution of eq iv and the fluorescence equivalents (eqs ii−v) into the equation for the second binding site results in the expression of fluorescence from site 2 (eq viii)

$$F_{(2)} = F_{o(2)} - K_{d1}K_{d2}L^2F_{(1)} \quad (viii)$$

Attributing the two fluroescence values (eqs vi and viii) to the equation for fluorescence (eq ii) and solving for the change in fluorescence yield the following relationship:

$$\frac{\Delta F}{F_o} = f_1\left(\frac{K_{d1}L + K_{d1}K_{d2}L^2}{1 + K_{d1}L}\right) \quad (2)$$

where f_1 is the fraction of enzyme which has ligand bound to site 1. If ligand does not bind site 2, or if the second site is indistinguishable from F_1, then eq 2 reduces to the equivalent of a single binding site (eq 1). Fluorescence quenching data were fit with eq 2 using nonlinear regression analysis (Kaleidagraph, Synergy Software), and fits for all variant acetate kinases are shown in Figure 4A−E, with good agreement between eq 2 and the experimental data. The K_d values for ATP·Mg and ADP·Mg determined from the fit for all double variants are listed in Tables 3 and 4. All

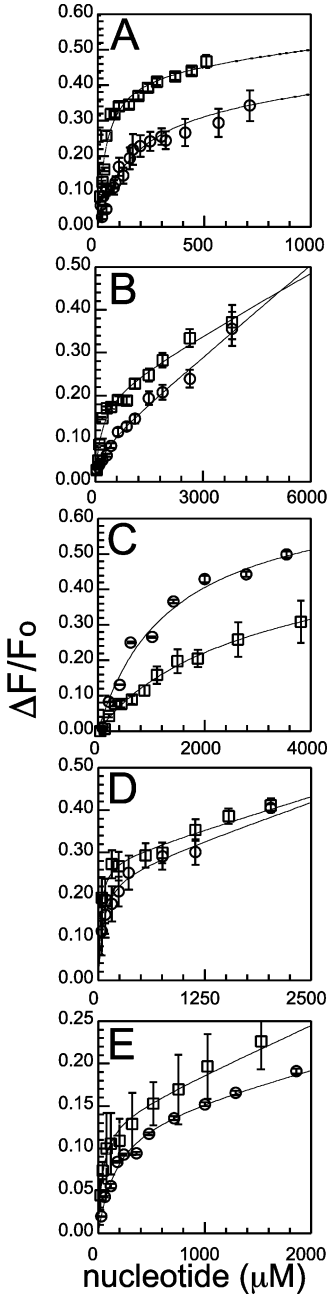

FIGURE 4: Nucleotide-dependent fluorescence quenching of acetate kinase variants: (A) $Gln^{43}Trp$ variant, (B) $Arg^{91}Ala/Gln^{43}Trp$ variant, (C) $Arg^{91}Lys/Gln^{43}Trp$ variant, (D) $Arg^{241}Ala/Gln^{43}Trp$ variant, and (E) $Arg^{241}Lys/Gln^{43}Trp$ variant. Symbols: ATP·Mg^{2+} (○) and ADP·Mg^{2+} (□).

Table 3: ATP·Mg^{2+} Binding Constants of Acetate Kinase Variants

variant	f_1	K_{d1} (μM)	K_{d2} (μM)
$Gln^{43}Trp$	0.45 ± 0.04	38.6 ± 8.2	5020 ± 1160
$Arg^{91}Ala/Gln^{43}Trp$	0.21 ± 0.03	167 ± 50	4506 ± 1200
$Arg^{91}Lys/Gln^{43}Trp$	0.44 ± 0.26	2190 ± 1600	35000 ± 12000
$Arg^{241}Ala/Gln^{43}Trp$	0.30 ± 0.02	30.7 ± 11	5400 ± 1100
$Arg^{241}Lys/Gln^{43}Trp$	0.15 ± 0.04	118 ± 90	2810 ± 1300

variants exhibited two dissociation constants (K_{d1} and K_{d2}) for the nucleotides, designated 1 for the tight binding site (K_{d1}) and 2 for the loose binding site (K_{d2}), and a f_1 value indicating the fraction of enzyme with ligand bound to the first site. The results indicate that the two binding sites in the dimeric acetate kinase can be distinguished. Since the enzyme is a homodimer, the results suggest that binding of substrate to one active site of the enzyme affects the ability of substrate to bind the opposing identical monomer, matching the description for a half-the-sites active enzyme.

Table 4: ADP·Mg^{2+} Binding Constants of Acetate Kinase Variants

variant	f_1	K_{d1} (μM)	K_{d2} (μM)
$Gln^{43}Trp$	0.39 ± 0.02	138 ± 5	7470 ± 1320
$Arg^{91}Ala/Gln^{43}Trp$	0.11 ± 0.02	221 ± 105	1360 ± 401
$Arg^{91}Lys/Gln^{43}Trp$	0.38 ± 0.05	193 ± 72	9140 ± 3200
$Arg^{241}Ala/Gln^{43}Trp$	0.25 ± 0.02	55.6 ± 13	3590 ± 490
$Arg^{241}Lys/Gln^{43}Trp$	0.19 ± 0.04	256 ± 94	4930 ± 2460

The K_{d1} values determined for both ATP and ADP (Tables 3 and 4) for the $Gln^{43}Trp$ variant are in agreement with the Michaelis constants for each nucleotide (Tables 1 and 2). The $K_{d1}^{ATP\cdot Mg}$ and $K_{d1}^{ADP\cdot Mg}$ values for both Arg^{241} double variants versus the $Gln^{43}Trp$ variant (Table 3) are not significantly different, indicating Arg^{241} has no role in binding either nucleotide.

Arg^{91} was previously postulated to have roles in stabilization of the *m*-phosphoryl transition state and orientation of acetate for catalysis with no role for binding ATP (*11*). Neither Arg^{91} double variant versus the $Gln^{43}Trp$ variant showed significant differences in the $K_{d1}^{ADP\cdot Mg}$ values (Table 4). The $Arg^{91}Ala/Gln^{43}Trp$ variant exhibited relatively little difference in $K_d^{ATP\cdot Mg}$ values versus the $Gln^{43}Trp$ variant (Table 3), consistent with no role in binding ATP. However, the $K_{d1}^{ATP\cdot Mg}$ for the $Arg^{91}Lys/Gln^{43}Trp$ variant was considerably larger than that of the $Gln^{43}Trp$ variant which contradicts the existing evidence. One possible explanation is that replacement of Arg^{91} with Lys interferes with domain closure which prevents fluorescence quenching.

DISCUSSION

Domain Motion. The analysis of nucleotide binding constants indicated that binding to one site affects binding to the other, suggesting a half-the-sites mechanism. Half-the-sites activity was first defined by Koshland as proteins of identical subunits where only one-half of the available sites are occupied in the presence of ligand (*26*) and theoretically described by Hill as concerted isologous dimers, where the two conformations of the dimer are always different, and the subunits change conformation in concert (*27*). Thus, the results presented here further suggest domain motion during catalysis by acetate kinase.

Acetate kinase has been classified as a member of the ASKHA structural superfamily (*12*) based upon the architectural organization; however, a second common feature of the superfamily members for which native and substrate-bound structures are available is a domain movement upon substrate binding (*13*). The best-characterized domain motion for catalytic activity is the domain closure of glycerol kinase, in which a sheer/sliding motion for domain closure for the ASKHA family has been defined (*28*). Domain motion in acetate kinase was postulated on the basis of the crystal structure (*12*) and supported by the kinetic characteristics of variants occurring at the domain I−II interface (Phe^{179}-Ala and $Leu^{122}Ala$) (*10*). The recent *Salmonella typhimurium* propionate kinase structure (*29*) again generated neither an open nor a closed structure, but an intermediate state in the catalytic mechanism. However, a model of domain motion based upon the small differences in the propionate kinase

and the *M. thermophila* acetate kinase structures suggested a potential change of ≤15 Å (*29*).

Fluorescence quenching occurs when the environment around a fluorescent moiety undergoes a change, resulting in the loss of the ability to release the absorbed energy as a lower-wavelength photon. Tryptophan fluorescence can be quenched when the environment changes from a hydrophobic to a hydrophilic environment. The assumption for the fluorescent acetate kinase is that a fluorescence change would occur upon ligand binding. The quenching observed experimentally is through one of two methodologies, one in which the nucleotide would directly interact with the engineered residue or one in which a change in conformation must occur. On the basis of the Gln^{43} side chain location buried in domain I, no direct interaction would be observed with a correctly folded protein. Thus, in the engineered acetate kinase, the tryptophan residue would fluoresce in the unbound (open) state and be quenched in the bound (closed) state, as a more hydrophobic environment is generated when domain I closed onto domain II. This was observed with the fluorescence quenching of the Gln^{43}Trp enzyme in the presence of the adenine nucleotides. Thus, the hypothesis that domain II closes onto domain I during acetate kinase activity upon nucleotide binding is supported, and this is the first direct evidence that supports a domain closure in the acetate kinase catalytic mechanism.

Kinetic and Dissociation Constants of the Double Variants. The kinetic and dissociation constants determined for the double variants clarify roles for Arg^{91} and Arg^{241}. The large decrease in k_{cat} for all double variants relative to Gln^{43}Trp supports the previously proposed roles for Arg^{91} and Arg^{241} in stabilization of the transition state by interaction with the *m*-phosphate based on kinetic analyses of variant enzymes (*11*).

The results presented here indicate that neither Arg is important for recognition and binding of either ATP or ADP, consistent with the previous proposal that adenine ring interactions are the major contributors to nucleotide recognition and binding (*12*). The f_1 value indicates that while one monomer is ligand-bound, the other is free, consistent with a half-the-sites mechanism. The results also indicate that while the arginines are not involved in the nucleotide recognition, a portion of the binding energy must contribute to closure of the domain, as the double variant enzymes all have a smaller f_1 than the Gln^{43}Trp variant. From the crystal structure, it is known that a distance of 7.1 Å (*11*) exists between the location of the Arg^{91} side chain and the *m*-phosphate analogue AlF_3 (Figure 1) which would require a substantial change for Arg^{91} to contact this phosphate and stabilize the transition state. The differential K_{d1}^{ADP} values for the Arg^{91}Ala/Gln^{43}Trp to Arg^{91}Lys/ Gln^{43}Trp variants with respect to the respective K_m^{ATP} and K_m^{ADP} values indicate a role in this conformational change. Thus, another role for Arg^{91} may be to facilitate domain closure driven by the energy of nucleotide binding that also positions Arg^{91} for interaction with this phosphate. The results suggesting that replacement of Arg^{91} with Lys interfered with domain closure are consistent with this proposal.

Implications for the Acetate Kinase Catalytic and Kinetic Mechanism. The nucleotide binding results, in conjunction with the known domain motion in the superfamily, suggest that domain closure occurs when substrate binds the active site which sequesters the substrates into a microenvironment where the arginine residues position the carboxyl group of acetate or the corresponding β-phosphate of ADP for nucleophilic attack on the γ-phosphate of ATP or phosphoryl group of acetyl phosphate. The implications for catalysis are that binding of the nucleotide induces a domain closure in that monomer and catalysis occurs in the closed active site. With active sites in each monomer, three possibilities exist for catalysis. First, the two active sites are independent of one another, and no coordination exists between the active sites of the two monomers. The results presented here indicated two nonidentical binding sites, which argues against this possibility. Second, the two active sites act in a coordinated fashion where both active sites are in the same state; i.e., ligand binding to one active site will cause domain closure in both active sites so both monomers are always in the same conformation (open and open or closed and closed only). The third possibility is that again the sites are coordinated, but when one active site is occupied and closed, the opposing monomer is in an open conformation (open and closed), the definition of the half-the-sites mechanism (*26*). As products are released from one site, the opposing site can now close, the dimer always having one occupied and one unoccupied site. The coordination can be postulated to occur by two mechanisms. In the first mechanism, once product is formed, substrate binding and subsequent domain closure of the opposite monomer contribute to the domain opening and release of product in the first active site. In the second, substrate is bound to the open active site and the release of product induces the closure of the opposing monomer which is already primed for activity. The highly divergent binding constants (K_{d1} vs K_{d2}) indicate that nucleotide substrates are not bound to both active sites concurrently, a result that argues against the first coordinated scheme (open and open) and supports the second (open and closed). Further investigation to distinguish between the two types of coordination in the acetate kinase mechanism is ongoing.

CONCLUSIONS

The binding constants for the nucleotide substrates indicate that Arg^{241} is involved in transition state stabilization and not directly involved in nucleotide recognition or binding, or in the domain closure required for catalysis. The binding constants of the nucleotide substrates for Arg^{91} suggest that this residue has a role in transition state stabilization. For the first time, evidence for domain motion dependent upon nucleotide ligand binding is presented for acetate kinase and suggests that Arg^{91} is important for closure of domain I onto domain II for catalysis. A scheme for coordinated activity between the two active sites in the dimer has been suggested, indicating that acetate kinase follows a half-the-sites activity and presents an avenue for further investigation into the coordination.

ACKNOWLEDGMENT

We thank Drs. Sarah H. Lawrence, Dan Lessner, and Stephen Rader for their critical reading of the manuscript.

REFERENCES

1. Ferry, J. G. (1997) Enzymology of the fermentation of acetate to methane by *Methanosarcina thermophila*, *Biofactors 6*, 25−35.

2. Lipmann, F. (1944) Enzymatic synthesis of acetyl phosphate, *J. Biol. Chem. 155*, 55−70.
3. Spector, L. B. (1980) Acetate kinase: A triple-displacement enzyme, *Proc. Natl. Acad. Sci. U.S.A. 77*, 2626−2630.
4. Blattler, W. A., and Knowles, J. R. (1979) Stereochemical course of phosphokinases. The use of adenosine [γ-(S)-^{16}O,^{17}O,^{18}O]-triphosphate and the mechanistic consequences for the reactions catalyzed by glycerol kinase, hexokinase, pyruvate kinase, and acetate kinase, *Biochemistry 18*, 3927−3933.
5. Purich, D. L., and Fromm, H. J. (1972) Evaluation of the phosphoryl-enzyme intermediate concept in the acetate kinase and hexokinase reactions from kinetic studies, *Arch. Biochem. Biophys. 149*, 307−315.
6. Miles, R. D., Gorrell, A., and Ferry, J. G. (2002) Evidence for a transition state analog, MgADP-aluminum fluoride-acetate, in acetate kinase from *Methanosarcina thermophila*, *J. Biol. Chem. 277*, 22547−22552.
7. Miles, R. D., Iyer, P. P., and Ferry, J. G. (2001) Site-directed mutational analysis of active site residues in the acetate kinase from *Methanosarcina thermophila*, *J. Biol. Chem. 276*, 45059−45064.
8. Singh-Wissmann, K., Ingram-Smith, C., Miles, R. D., and Ferry, J. G. (1998) Identification of essential glutamates in the acetate kinase from *Methanosarcina thermophila*, *J. Bacteriol. 180*, 1129−1134, 3018 (erratum).
9. Singh-Wissmann, K., Miles, R. D., Ingram-Smith, C., and Ferry, J. G. (2000) Identification of essential arginines in the acetate kinase from *Methanosarcina thermophila*, *Biochemistry 39*, 3671−3677.
10. Ingram-Smith, C., Gorrell, A., Lawrence, S. H., Iyer, P., Smith, K., and Ferry, J. G. (2005) Characterization of the acetate binding pocket in the *Methanosarcina thermophila* acetate kinase, *J. Bacteriol. 187*, 2386−2394.
11. Gorrell, A., Lawrence, S. H., and Ferry, J. G. (2005) Structural and kinetic analyses of arginine residues in the active site of the acetate kinase from *Methanosarcina thermophila*, *J. Biol. Chem. 280*, 10731−10742.
12. Buss, K. A., Cooper, D. C., Ingram-Smith, C., Ferry, J. G., Sanders, D. A., and Hasson, M. S. (2001) Urkinase: Structure of Acetate Kinase, a Member of the ASKHA Superfamily of Phosphotransferases, *J. Bacteriol. 193*, 680−686.
13. Hurley, J. H. (1996) The sugar kinase/heat shock protein 70/actin superfamily: Implications of conserved structure for mechanism, *Annu. Rev. Biophys. Biomol. Struct. 25*, 137−162.
14. Feese, M. D., Faber, H. R., Bystrom, C. E., Pettigrew, D. W., and Remington, S. J. (1998) Glycerol kinase from *Escherichia coli* and an Ala65 → Thr mutant: The crystal structures reveal conformational changes with implications for allosteric regulation, *Structure 6*, 1407−1418.
15. Fung, K. L., Hilgenberg, L., Wang, N. M., and Chirico, W. J. (1996) Conformations of the nucleotide and polypeptide binding domains of a cytosolic Hsp70 molecular chaperone are coupled, *J. Biol. Chem. 271*, 21559−21565.
16. Gerstein, M., Schulz, G., and Chothia, C. (1993) Domain closure in adenylate kinase. Joints on either side of two helices close like neighboring fingers, *J. Mol. Biol. 229*, 494−501.
17. Liu, W. Z., Faber, R., Feese, M., Remington, S. J., and Pettigrew, D. W. (1994) *Escherichia coli* glycerol kinase: Role of a tetramer interface in regulation by fructose 1,6-bisphosphate and phosphotransferase system regulatory protein IIIglc, *Biochemistry 33*, 10120−10126.
18. Page, R., Lindberg, U., and Schutt, C. E. (1998) Domain motions in actin, *J. Mol. Biol. 280*, 463−474.
19. Aceti, D. J., and Ferry, J. G. (1988) Purification and characterization of acetate kinase from acetate-grown *Methanosarcina thermophila*. Evidence for regulation of synthesis, *J. Biol. Chem. 263*, 15444−15448.
20. Kunkel, T. A., Roberts, J. D., and Zakour, R. A. (1987) Rapid and efficient site-specific mutagenesis without phenotypic selection, *Methods Enzymol. 154*, 367−382.
21. Latimer, M. T., and Ferry, J. G. (1993) Cloning, sequence analysis, and hyperexpression of the genes encoding phosphotransacetylase and acetate kinase from *Methanosarcina thermophila*, *J. Bacteriol. 175*, 6822−6829.
22. Laemmli, U. K. (1970) Cleavage of structural proteins during the assembly of the head of bacteriophage T4, *Nature 227*, 680−685.
23. Bradford, M. M. (1976) A rapid and sensitive method for the quantitation of microgram quantities of protein utilizing the principle of protein-dye binding, *Anal. Biochem. 72*, 248−254.
24. Allen, S., Kellermeyer, R., Stjernholm, R., and Wood, H. (1964) Purification and Properties of Enzymes Involved in the Propionic Acid Fermentation *J. Bacteriol. 87*, 171−187.
25. Lakowicz, J. R. (1999) *Principles of fluorescence spectroscopy*, 2nd ed., Kluwer Academic/Plenum, New York.
26. Levitzki, A., Stallcup, W. B., and Koshland, D. E., Jr. (1971) Half-of-the-sites reactivity and the conformational states of cytidine triphosphate synthetase, *Biochemistry 10*, 3371−3378.
27. Hill, T. L. (1978) Unsymmetrical and concerted examples of the effect of enzyme−enzyme interactions on steady-state enzyme kinetics, *Proc. Natl. Acad. Sci. U.S.A. 75*, 1101−1105.
28. Bystrom, C. E., Pettigrew, D. W., Branchaud, B. P., O'Brien, P., and Remington, S. J. (1999) Crystal structures of *Escherichia coli* glycerol kinase variant S58→W in complex with nonhydrolyzable ATP analogues reveal a putative active conformation of the enzyme as a result of domain motion, *Biochemistry 38*, 3508−3518.
29. Simanshu, D. K., Savithri, H. S., and Murthy, M. R. (2005) Crystal structures of ADP and AMPPNP-bound propionate kinase (TdcD) from *Salmonella typhimurium*: Comparison with members of acetate and sugar kinase/heat shock cognate 70/actin superfamily, *J. Mol. Biol. 352*, 876−892.

BI701292A